Journal of Engineering Physics and Thermophysics, Vol. 80, No. 6, 2007

HYDRODYNAMIC DESCRIPTION OF THE MECHANISM OF FORMATION OF CARBON NANOTUBES

G. V. Abramov, A. I. Ivanov, and G. V. Popov

UDC 533.95:544.272

The electric-arc process of synthesis of carbon nanotubes has been investigated with the aim of searching for the mechanical trajectories of the ionic component of a carbon arc plasma and evaluating their influence on the formation of carbon nanotubes on the cathode. The conclusion on the predominantly ionic composition of the plasma has been drawn on the basis of experimental study of the degree of ionization. It has been proposed that a magnetohydrodynamic model be used for description of the motion of the charged component. The calculated region of the predominant accumulation of carbon ions has been compared to the actual distribution of carbon nanotubes.

Introduction. The electric-arc method of synthesis of carbon nanotubes is accepted as the most efficient one by some authors [1]. When it is used, the graphite anode burns out and the deposit on the cathode grows. The parameters of the process for synthesis of carbon nanotubes — helium pressure in the chamber of the order of 500 Torr, distance between the electrodes 1 mm, current strength in the circuit 100 A, and electrode diameter of 5 to 20 mm — have been revealed during the investigations [1–3].

The structural composition of the deposit is heterogeneous. It is dominated by three allotropic carbon states: fullerenes, nanotubes, and amorphous soot-like carbon. These fractions are detected by electronic microscopy and x-ray structural analysis. Such a variety of deposit fractions is formed from a carbon plasma containing (as most researchers note [1–3]) a charged component — carbon ions — and a neutral component — carbon atoms and carbon clusters.

An analysis of publications shows that we can single out several viewpoints as far as the mechanism of formation of carbon nanotubes is concerned. In [1, 3], the formation of nanotubes is attributed to the combination of carbon clusters. In the cathode region, they interact with each other, seeking to eliminate free edge carbon bonds by uniting into fullerenes and nanotubes.

According to the Gamaly and Ebbesen theory [2], in the cathode region, there is a "vapor layer" of carbon ions with a Maxwelian velocity distribution. These particles form amorphous asymmetric structures. The penetration of a directed anode particle flux into the vapor layer leads to an elongation of nanotubes; the layer is involved in their thickening.

The absence of a unified viewpoint as far as the process of synthesis is concerned is primarily due to the problems of experimental study of these phenomena. The high temperature of the plasma (no less than 4000 K [1]) and the transient nature of the processes in it make it impossible to investigate the formation of nanotubes by direct experimental methods.

In this work, we seek to determine the mechanical trajectories of the charged plasma component on the basis of mathematical modeling of the phenomena.

The well-known theories of Gamaly and others considering the plasma in the context of empiricism involve a number of uncertainties. For example, in calculating the ordered motion of ions, no account is taken of the collisions in the plasma, and the ion velocity is taken to be of about 18 km/sec, which is inconsistent with the experimental data of other authors, e.g., Volchenko et al. [4]. The interaction of the flux with electromagnetic fields and the presence of the neutral component are not considered.

Voronezh State Academy of Technology, 19 Prospekt Revolutsii, Voronezh, 394000, Russia; email: pgw@vgta.vrn.ru. Translated from Inzhenerno-Fizicheskii Zhurnal, Vol. 80, No. 6, pp. 49–56, November–December, 2007. Original article submitted April 11, 2006; revision submitted December 14, 2006.

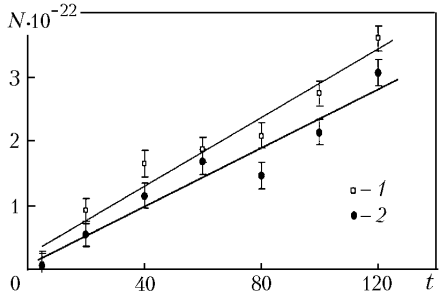

Fig. 1. Relation of the number of atoms transferred by the arc as a function of the duration of the experiment (the number of parallel experiments is no less than four): 1) calculation from the transferred mass; 2) calculation from the traversed charge. t, sec.

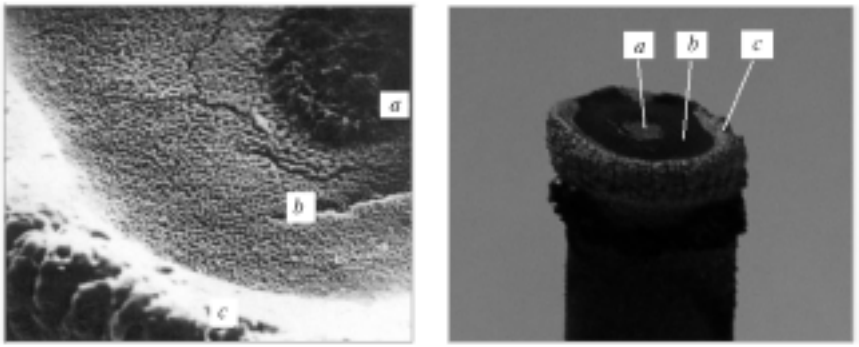

Fig. 2. View of the deposit surface (on the left, magnified view of the surface, obtained in [6]; on the right, characteristic view of the deposit on the cathode): a) central zone; b) surface with randomly arranged floccular granules; c) external boundary of the deposit in the form of a barrier.

Modeling of the Electric-Arc Synthesis of Carbon Nanotubes. The authors have performed experimental evaluation to substantiate the approach to mathematical modeling and to reveal the structure of the plasma flow. The current and the deposit mass were measured during the experiment at different synthesis times. It was assumed that carbon ions in the discharge plasma are simultaneously charge and mass carriers and a companion of the deposit mass to the current during the experiment makes it possible to determine the degree of ionization. With allowance for the quasineutrality characteristic of the given plasma, the degree of ionization can be evaluated by the formula [5]

$$\alpha = \frac{N_{\mathrm{i}}}{N_{\mathrm{t}}} = \frac{I \Delta t m_{\mathrm{i}}}{2 \Delta m Z q_{\mathrm{i}}} . \tag{1}$$

From the results of processing of the experimental run (Fig. 1), evaluation of the degree of ionization under conditions corresponding to the synthesis of carbon nanotubes yields α = 65–85%. Consequently, more than 60% of the deposit mass is formed due to the ionized material. The radial nonuniformity of the deposit (Fig. 2) described by many authors [1, 6] has been confirmed during the experiments. Representing the discharge as a narrow "plasma core" heating the ambient gas, we cannot explain the presence of three zones of the deposit within the framework of a classical arc-discharge theory [4].

From the data of [1, 6], the zones have different contents of nanotubes. Clearly, the mechanical trajectories of charged and uncharged particles in the plasma will be different. The reason is the presence of electric and magnetic forces acting under arc-discharge conditions. Modeling of the mechanical trajectories of the plasma components makes it possible to evaluate the mechanism of formation of nanotubes on the cathode. When only two plasma components

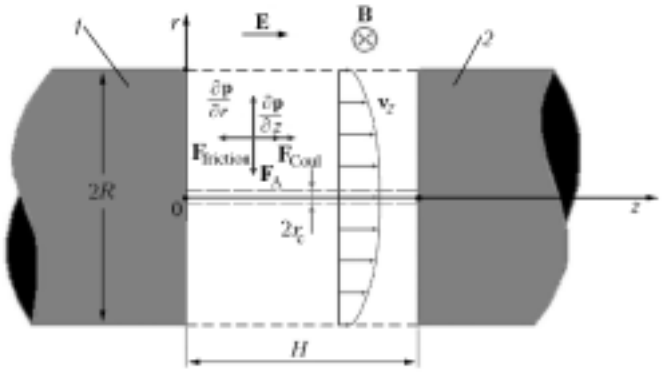

Fig. 3. Computational scheme of the process: 1) anode; 2) cathode.

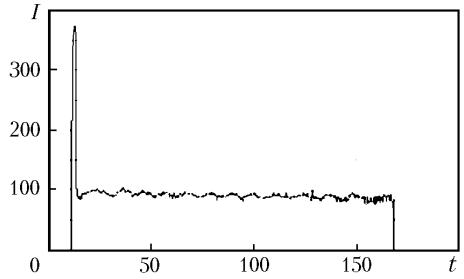

Fig. 4. Oscillogram of stable arcing (the constancy of the current is maintained by bringing the electrodes together). *I*, A; *t*, sec.

are present, it is sufficient to find the concentration region of one component and to compare to the actual distribution of carbon nanotubes.

We know of different methods of describing phenomena in the plasma: drift theory and magnetohydrodynamic and kinetic descriptions. From the viewpoint of the authors, the magnetohydrodynamic approach is the best for solution of this problem, since it enables one to obtain the mechanical trajectories of charged particles and to relate the parameters of the deposit, the electrodes, and the plasma. On the basis of what has been said above and taking into account that evaluation of the degree of ionization has shown the predominance of the ionic component, we propose that its precise motion be described using magnetohydrodynamic equations. In this case, a computational scheme can be represented in the form of Fig. 3.

A distinctive feature of the process of synthesis of carbon nanotubes is plasma flow in a short gap between the anode and the cathode — relation of the gap length and the electrode diameter $H/2R \approx 1/10$. With allowance for this fact, the initial system of equations [5]

$$\frac{\partial \rho}{\partial t} + \operatorname{div}(\rho \mathbf{v}) = 0\,, \quad \rho \frac{d\mathbf{v}}{dt} = \mathbf{F}_{\text{Coul}} + \mathbf{F}_{\text{A}} - \nabla \mathbf{p} + \mu \nabla^2 v\,, \quad \operatorname{div} \mathbf{D} = \rho_{\text{fr}}\,, \quad \operatorname{rot} \mathbf{H}_{\text{m}} = \mathbf{j} + \frac{\partial \mathbf{D}}{\partial t}\,, \quad \operatorname{div} \mathbf{B} = 0\,,$$

$$\operatorname{rot} \mathbf{E} = -\frac{\partial \mathbf{B}}{\partial t}\,, \quad \mathbf{j} = \rho \mathbf{v} k\,, \quad \mathbf{D} = \varepsilon \mathbf{E}\,, \quad \mathbf{B} = \mu_{\text{m}} \mathbf{H}_{\text{m}} \tag{2}$$

will substantially be simplified due to the uniformity of the elastic and magnetic fields.

Solution of Eqs. (2) in their initial form is possible just for a small class of problems. The difficulty here is in the presence of nonlinearity in the convective terms and in determining constants: dynamic viscosity, permeability and permittivity of the medium, and others.

A number of assumptions have been made to obtain approximate solutions. An analysis of the current oscillogram (Fig. 4) in the process of synthesis makes it possible to draw a conclusion on the rapid attenuation of the tran-

sient processes; consequently, the process of synthesis can be considered as being stationary and $\partial/\partial t \equiv 0$. The experiments show the axial symmetry at the process (Fig. 2).

Using the cylindrical coordinate system for modeling, with allowance for the symmetry we can write that $v_\varphi = 0$, $\partial v_r/\partial\varphi = 0$, $\partial v_z/\partial\varphi = 0$, $\partial \mathbf{D}/\partial\varphi = 0$, and $\partial \mathbf{B}/\partial\varphi = 0$, i.e., we have $B_\varphi(\varphi) = \text{const} = B$. Then all projections of the vectors are functions of two variables z and r.

The electric-field vector can be considered to be orthogonal to the electrode surface and to be constant at each point; consequently, we have $E_r = 0$, $E_\varphi = 0$, and $E_z = \text{const} = E$.

Assuming that the temperature changes only slightly in the region in question, we take $\mu(T) = \text{const}$. Clearly, charge separation will occur in the plasma under the action of electromagnetic forces, which will cause the plasma density to change; then we will have $\rho = \rho(z, r)$.

On the basis of the computational scheme and the assumptions made, the system of initial equations will take the form

$$\frac{\partial j_r}{\partial r} + \frac{\partial j_z}{\partial z} + \frac{j_r}{r} = 0 , \tag{3}$$

$$\rho v_r \frac{\partial v_z}{\partial r} + \rho v_z \frac{\partial v_z}{\partial z} = E\rho k - \frac{\partial p}{\partial z} + \mu\left(\frac{\partial^2 v_z}{\partial z^2} + \frac{\partial^2 v_z}{\partial r^2} + \frac{1}{r}\frac{\partial v_z}{\partial r}\right), \tag{4}$$

$$\rho v_r \frac{\partial v_r}{\partial r} + \rho v_z \frac{\partial v_r}{\partial z} = j_z B - \frac{\partial p}{\partial z} + \mu\left(\frac{\partial^2 v_r}{\partial z^2} + \frac{\partial^2 v_r}{\partial r^2} + \frac{1}{r}\frac{\partial v_r}{\partial r} - \frac{v_r}{r^2}\right) \tag{5}$$

$$j_z = v_z \rho k , \tag{6}$$

$$j_r = v_r \rho k , \tag{7}$$

$$j_z = \frac{1}{\mu_m r}\left(\frac{\partial (Br)}{\partial r}\right), \tag{8}$$

$$j_r = -\frac{1}{\mu_m}\left(\frac{\partial B}{\partial z}\right). \tag{9}$$

Here the charge equation is used instead of the continuity equation for convenience of solution.

We introduce the core of radius r_c at the center of the flow into consideration; temperature and pressure in the core are assumed to be constant. Boundary conditions for system (3)–(9) for $r = r_c$ follow from the symmetry condition: $v_r = 0$, $j_r = 0$, $B = 0$, and $v_z = f(z)$.

To solve system (3)–(9) we introduce the current function $i(z, r)$ such that

$$j_z = \frac{\partial i}{\partial S} . \tag{10}$$

This makes it possible to diminish the number of unknowns in system (3)–(9) by expressing the current density j_r by the current function from Eq. (3) and the magnetic induction B from Eqs. (8) and (9) and to relate the axial and radial velocities in Eqs (6) and (7) by the current function.

The above transformations enable us to seek the approximate solution of system (3)–(9) for the functions v_z, i, and p in the form of the series

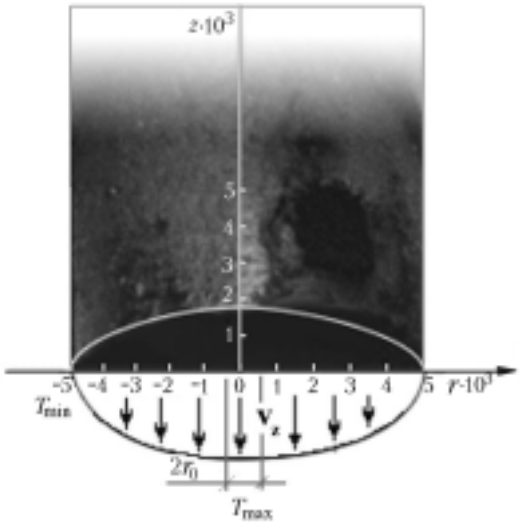

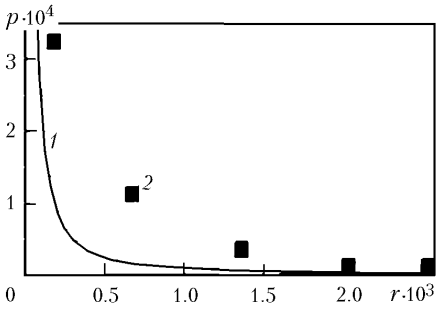

Fig. 5. Profile of anode burnout at the 80th second of the experiment; the high velocity of particles at the center is a result of the higher temperature (>400 K) [4, 7].

Fig. 6. Radial pressure distribution in the cathode region for a current of 100 A (comparison of the calculated (1) and experimental (2) data obtained in [8]). p, Pa; r, m.

$$i = \sum_{n=0}^{m_1} \xi^n i_n(r), \quad v_z = \sum_{n=0}^{m_2} \xi^n v_n(r), \quad p = \sum_{n=0}^{m_3} \xi^n p_n(r), \tag{11}$$

where $\xi = z/H$. Checking the convergence of system (3)–(9) has shown that we can restrict ourselves to the values $m_1 = 2$, $m_2 = 2$, and $m_3 = 1$ with a sufficient degree of accuracy.

Substituting the functions (11) into the equations of motion (4) and (5), we find a system of equations explicitly dependent on z and including the unknown functions: $v_0(r)$, $v_1(r)$, $v_2(r)$, $i_0(r)$, $i_1(r)$, $i_2(r)$, $p_0(r)$, and $p_1(r)$.

By algebraic transformations we obtain, from system (3)–(9), the equivalent system

$$\frac{d}{dr} v_2(r) = W_2(r), \quad \frac{d}{dr} v_1(r) = W_1(r), \quad \frac{d}{dr} i_2(r) = \frac{i_2(r) W_2(r)}{v_2(r)}, \quad \frac{d}{dr} i_1(r) = \frac{i_2(r) W_2(r) v_1(r)}{v_2(r)^2},$$

$$\frac{d}{dr} i_0(r) = -\frac{V i_2(r) W_2(r) (-R^2 + r^2)}{v_2(r)^2 R^2}, \quad \frac{d}{dr} W_2(r) = f_1(v_1(r), v_2(r), i_1(r), i_2(r), W_1(r), W_2(r)), \tag{12}$$

$$\frac{d}{dr} W_1(r) = f_2(v_1(r), v_2(r), i_1(r), i_2(r), W_1(r), W_2(r)),$$

$$\frac{d}{dr} p_0(r) = f_3(v_1(r), v_2(r), i_0(r), i_1(r), i_2(r), W_1(r), W_2(r)).$$

Boundary conditions to system (12) can be formulated with allowance for the profile of anode burnout (Fig. 5). This makes it possible to prescribe the velocity at the boundary $z = 0$ as $v_0(r) = V(1 - (r/R)^2)$. Here we have $V = v_z(0, 0) \approx 100$ m/sec [4, 5]. Clearly, the value of the current function at the anode is $i_0(R) = 50$ A, $W_1(R) = dv_1/dr\,|_{r=R} \approx -10^7$ 1/sec [4], and $p_0(R) = 6.5 \cdot 10^4$ Pa is the helium pressure in the chamber. The values of the constants are $\mu_m = 1.3 \cdot 10^{-6}$ H/m, $E = 2 \cdot 10^4$ V/m, and $k = 0.8 \cdot 10^7$ C/kg.

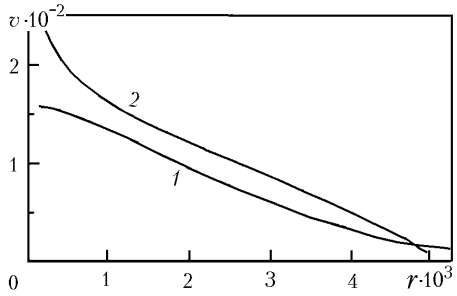

Fig. 7. Radial axial-velocity distribution in the cathode region: 1) calculated distribution; 2) distribution obtained in [9]. *r*, m; *v*, m/sec.

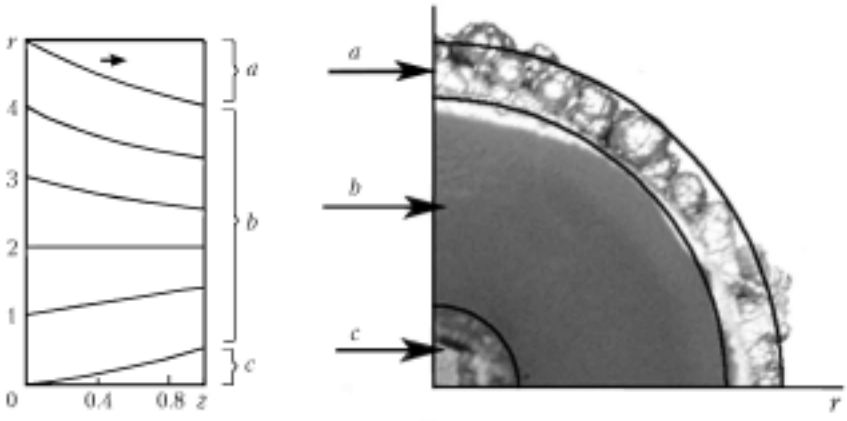

Fig. 8. Formation of the regions with different ion concentrations on the deposit: a) central region, a low content of ions; b) middle, the highest concentration of ions; c) peripheral region, the lowest concentration of carbon ions. *r* and *z*, m.

The lacking numerical values in the boundary conditions are found by the successive simplex method and minimization of the "desirability function," representing the difference squared of experimental and calculated currents.

The adequacy of the model has been checked by comparing the pressure and velocity distribution according to the model to the results of other authors. To compare to the results of [8] we calculated the model for a vacuum arc discharge for a current of 100 A and an electrode spacing of H = 3 mm. The results are presented in Fig. 6 and show that the calculated and experimental values are fairly close. Figure 7 compares the axial-velocity distributions to the results of [9] (current I = 300 A and H = 1 mm) for an argon arc.

From the found projections of velocity for steady-state flow, we have constructed the mechanical trajectories of charged plasma particles for different points of the anode (Fig. 8). The presence of nanotubes in zone *b* was confirmed by the x-ray structural investigations carried out and by investigation with a tunnel electron microscope. To study the radial distribution of nanotubes we took samples of equal mass in three zones of the deposit. The analysis results (Fig. 9) have shown that the relative number of nanotubes with an interlayer distance d_{002} = 0.343 nm in zone *b* is larger than that in zone *a* (see [10, 11] for the analysis of the x-ray photographs of nanotubes). In zone *c*, we only found graphite d_{002} = 0.339 nm. The concentration of carbon nanotubes in the region of predominant ion concentration enables us to draw the conclusion that ions are involved in the formation of nanotubes.

The influence of the plasma temperature on the synthesis of carbon nanotubes can be evaluated by the model's parameters, such as the coefficient of dynamic viscosity, the density, and the pressure. The stability of the hydrodynamic model to the change in the value of the relative area of region *b* (ion-concentration zone) was evaluated by varying the parameters. It has been established that the area of this region changes with considerable variation of

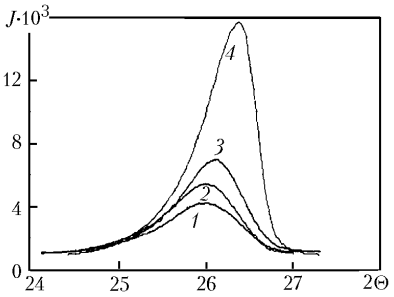

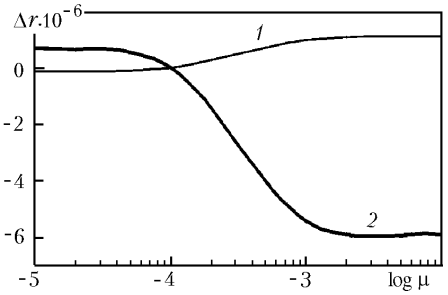

Fig. 9. Diffraction patterns of the samples in the region of the principal diffraction maximum [002]: 1) central region of the deposit *a*, d_{002} = 0.343 nm; 2) middle of the deposit, region *b*, d_{002} = 0.343 nm; 3) periphery of the deposit, zone *c*, d_{002} = 0.339 nm; 4) pure graphite, d_{002} = 0.337 nm. *J*, pulses/sec; Θ, deg.

Fig. 10. Increase in the boundaries of zone *b* with variations in the coefficient of viscosity (calculated from the model): 1) boundary between zones *a* and *b*; 2) boundary between zones *b* and *c*. Δ*r*, m; μ, Pa·sec.

the parameters only slightly, e.g., with considerable variations of the coefficient of dynamic viscosity, the variation of the relative area amounted to no more than 0.5% (Fig. 10), which confirms the stability of the model.

This work was carried out with support from the Russian Foundation for Basic Research, grant No. 06-08-01310.

CONCLUSIONS

1. On the basis of the experiments, we have found the ratio of the charged and uncharged components in the carbon plasma. The degree of ionization amounts to 65–85% under conditions corresponding to the formation of nanotubes. It is most expedient to select the magnetohydrodynamic approach for mathematical description of plasma flow.

2. We have established the mechanical trajectories of carbon ions and have determined the region of their most probable arrival, whose boundaries were coincident with the region of the highest concentration of carbon nanotubes. From the model obtained, we can predict the dimensions of the zone of accumulation of nanotubes, assigning the design parameters of electric-arc-synthesis devices.

NOTATION

B, B_z, B_r, and B_φ, magnetic-inductance vector and its components, T; d_{002}, interplanar spacing in the direction [002], nm; **D**, electric-inductance vector, C/m^2; **E**, E_z, E_r, and E_φ, electric-field vector and its components, V/m; $\mathbf{F}_A$, Ampere force, N; $\mathbf{F}_{friction}$, viscous-friction force per unit volume, N/m^3; $\mathbf{F}_{Coul}$, Coulomb force per unit volume, N/m^3; *H*, electrode-spacing length, m; **H**, H_z, H_r, and H_φ, magnetic-field vector and its components, H; *I*, total current through the electrode spacing, A; *i*, ionic-current function, A; *J*, x-ray radiation intensity, pulses/sec; **j**, j_z, j_r, and j_φ, vector of ionic-current density and its components, A/m^2; *k*, coefficient expressing the ratio of the particle charge to the particle mass for a singly charged carbon ion $k = q_i/m_i = 0.8 \cdot 10^7$ C/kg; m_i, carbon atomic mass, kg; *m*, deposit mass, kg; Δ*m*, increase in the cathode mass during the experiment, kg; *N*, number of atoms; N_t, total number of carbon atoms and ions in the plasma; N_i, number of carbon ions in the plasma; $\nabla\mathbf{p}$, pressure gradient, N/m^3; *p*, pressure, Pa; q_i, ionic charge, C; *r*, dimensional radial coordinate, m; Δ*r*, increase in the dimension of the boundaries of the ion-concentration zone, m; r_c, radius of the plasma core, m; *R*, electrode radius, m; $S = \pi r^2$, element of the area of radius *r*, m^2; Δ*t*, experimental time, sec; *t*, running experimental time, sec; *T*, plasma temperature, K; **v**, v_z, v_r, and v_φ, vector of the velocity of ordered motion of carbon ions and its components in the cylindrical coordinate system (z, r, φ), m/sec; *V*, velocity at the center of the anode, m/sec; *W*, radial axial-velocity gradient, 1/sec; *z*, dimensional axial coordinate, m; *Z*, average plasma charge, under nanotube-synthesis conditions, Z = 1.4;

α, degree of ionization of the plasma, %; ε, permittivity of the medium, F/m; φ, tangential coordinate; μ_m, permeability of the medium, H/m; μ, dynamic viscosity, Pa·sec; Θ, diffraction angle of x rays, deg; ρ_{fr}, volume density of free charge in the plasma, C/m^3; ρ, plasma density, kg/m^3; ξ, dimensionless axial coordinate. Subscripts: 0, 1, and 2, coefficients of the power series; i, ion; Coul, Coulomb; m, magnetic; t, total; fr, free; friction, friction; el, electron; c, core; *n*, ordinal No. of the term of the power series; max, maximum; min, minimum.

REFERENCES

1. P. J. F. Harris, *Carbon Nanotubes and Related Structures: New Materials for the Twenty-first Century* [Russian translation], Tekhnosfera, Moscow (2003).
2. E. G. Gamaly and T. W. Ebbesen, Mechanism of carbon nanotube formation in the arc discharge, *Phys. Rev. B*, **52**, No. 3, 2083–2089 (1995).
3. A. V. Eletskii, Carbon nanotubes and their emission properties, *Usp. Fiz. Nauk*, **172**, No. 4, 401–438 (2002).
4. V. N. Volchenko, B. M. Yampol'skii, and V. V. Frolova, *Theory of Welding Processes* [in Russian], Vysshaya Shkola, Moscow (1988).
5. A. I. Ivanov and G. V. Popov, Hydrodynamic description of the dynamics of synthesis of carbon nanotubes, in: *Proc. 12th Int. Symp. "Dynamic and Technological Problems of the Mechanics of Structures and Continua"* [in Russian], MAI (2006), pp. 163–165.
6. I. V. Zolotukhin, I. M. Golev, E. K. Belonogov, et al., Structure and thermal e.m.f. of a nanotube carbon deposit obtained in the electric-discharge plasma, *Pis'ma Zh. Tekh. Fiz.*, **29**, Issue 23, 84–90 (2003).
7. S. N. Aksenov, S. V. Ershov, G. V. Popov, et al., Prerequisites for controlling the synthesis of carbon nanotubes, in: *Proc. 6th Int. Conf. "Cybernetics and High Technologies"* [in Russian], VGU, Voronezh (2003), pp. 575–579.
8. V. A. Birzhev, A. V. Chernykh, and D. E. Kucher, Analysis of the thermodynamic nature of plasma fluxes in welding arcs, in: *Collected Reports of the Voronezh State Technical University* [in Russian], VGTU, Voronezh (2000), pp. 68–72.
9. V. S. Mechev, A. Zh. Zhainakov, M. A. Samsonov, et al., Plasma fluxes in welding arcs, *Avtomatich. Svarka*, No. 12, 13–16 (1981).
10. B. P. Tarasov, V. E. Muradyan, and Yu. M. Shul'ga, Investigation of the products of electric-arc vaporization of metal-graphite electrodes, *International Scientific Journal for Alternative Energy and Ecology* (*ISJAEE*), No. 6, 4–11 (2002).
11. Yu. M. Shul'ga, D. V. Shchur, A. P. Mukhachev, et al., Study of cathode deposits formed on electric arc sputtering of Zr–M graphite electrodes, in: *Proc. Int. Conf. "Hydrogen Materials Science and Chemistry of Carbon Materials,"* ISHMS-2003 [in Russian], Sudak, Ukraine (2003), pp. 452–453.